Modelling the Neutron Star

Hojae Lim

10825498

School of Physics and Astronomy

University of Manchester

Theory Computing Project

April 2023

Abstract

We have modelled the distribution of pressure and density as a function of the radius for neutron stars by computationally solving coupled ordinary differential equations. This was mainly done through the usage of the Runge-Kutta algorithm and the secant method in Python. The equations were solved under various assumptions, namely the polytropic, polytropic with Tolman-Oppenheimer-Volkoff (TOV) correction and the fully relativistic case. The neutron star with the largest mass for the fully relativistic case was found at core pressure $p_0 = 3.6 \cdot 10^{34}$ Pa, with radius R = 9.14 km and mass M = 0.71 $M_\odot$.

1 Introduction

Neutron stars are created by a Type II supernova, from the collapse of giant stars ($> 8M_\odot$), and are one of the densest objects in the universe [1]. Although it does partly contain protons and electrons, the primary composition of the star is neutrons, hence the name.

In this paper, we will attempt to model the neutron star distribution of pressure and density as a function of the radius. This will be done through solving coupled ordinary differential equations, under different assumptions, such as the polytropic equations of state and the fully relativistic case. Python will be the language in use, along with the libraries NumPy [2], SciPy [3] and Matplotlib [4].

2 Theory

In this section, we discuss the theoretical aspect of the physics used with the modelling, particularly summarising the formalism outlined in ref. [5] by Sagert et al.

We start by using the hydrostatic equilibrium, as we are modelling a stable neutron star, which is composed of Fermi neutron gas (Fermi electron gas for white dwarfs):

$$\frac{dp}{dr} = -\frac{G\rho(r)m(r)}{r^2}, \tag{2.1}$$

where G is the gravitational constant, ρ is the density, m is the mass and r is the radius. We also know that matter enclosed in a spherical shell can be described by:

$$m(r) = \int_0^r \rho(r')4\pi(r')^2\, dr', \tag{2.2}$$

so we can rewrite this into a differential equation:

$$\frac{dm}{dr} = \rho(r)4\pi r^2. \tag{2.3}$$

These are the fundamental coupled differential equations we will use throughout this paper.

2.1 The Polytropic Case

Let us first explore the polytropic assumption. The polytropic equation of state is [6]:

$$p = K\epsilon^{(n+1)/n}, \tag{2.4}$$

where K is the constant of proportionality and n is the polytropic index. These constants are different depending on the situation. For example, in the case of non-relativistic neutron stars, $n = 1.5$ (this value is more suitable for larger stars, but for consistency with white dwarfs we will use this value throughout this paper - a more appropriate value would be $n = 0.5 \sim 1$; [6, 7]) and

$$K = \frac{\hbar^2}{15\pi^2 m_n}\left(\frac{3\pi^2}{m_n c^2}\right)^{5/3}. \tag{2.5}$$

Throughout this paper, we will use $\gamma = (n+1)/n$ instead for simplicity. Further explanation on how the polytropic equation is defined is in section 2.4. Rearranging eq. (2.4) and substituting ϵ into equations (2.1) and (2.3), we get:

$$\frac{dp(r)}{dr} = -\frac{R_0 p(r)^{1/\gamma}\bar{\mathrm{m}}(r)}{r^2 K^{1/\gamma}}, \tag{2.6}$$

$$\frac{d\bar{\mathrm{m}}(r)}{dr} = \frac{4\pi r^2}{\mathrm{M}_\odot c^2}\left(\frac{p(r)}{K}\right)^{1/\gamma}, \tag{2.7}$$

where $\bar{\mathrm{m}} = m/\mathrm{M}_\odot$, $\mathrm{M}_\odot$ being the solar mass.

2.2 The Chandrasekhar Limit

2.2.1 Derivation of the Lane-Emden Equation

Note that the derivation follows the path of reference [5], but with more detail. We start with the two equations eq. (2.1) and eq. (2.3). We can deform eq. (2.1) into

$$\frac{1}{\rho}\frac{dp}{dr} = -\frac{Gm}{r^2},$$

where we can differentiate both sides and use eq. (2.3) to find

$$\begin{aligned}\frac{d}{dr}\left(\frac{1}{\rho}\frac{dp}{dr}\right) &= \frac{2Gm}{r^3} - \frac{G}{r^2}\frac{dm}{dr} \\ &= -\frac{2}{\rho r}\frac{dp}{dr} - 4\pi G\rho.\end{aligned} \tag{2.8}$$

With some rearranging and simple algebraic manipulation, we find that

$$\frac{d}{dr}\left(\frac{r^2}{\rho}\frac{dp}{dr}\right) = -4\pi G r^2 \rho.$$

Using the polytropic assumption from eq. (2.4), we find that

$$\frac{dp}{dr} = K\gamma\rho^{\gamma-1}c^{2\gamma}\frac{d\rho}{dr}.$$

Now, defining a new variable

$$\rho(r) = \rho_0\theta^n, \quad \theta \equiv \theta(r) \tag{2.9}$$

where ρ_0 is the central density and θ is the 'dimensionless density', we can use this to find

$$\frac{d\rho}{dr} = \rho_0 n\theta^{n-1}\frac{d\theta}{dr}.$$

Substituting dp/dr and $d\rho/dr$ into eq. (2.8), we find

$$\frac{1}{r^2}\frac{d}{dr}\left(r^2 K(1+n){\rho_0}^{1/n}\frac{d\theta}{dr}c^{2\gamma}\right) = -4\pi G\rho_0\theta^n. \tag{2.10}$$

We also define

$$r = a\xi, \quad \text{where} \quad a = \left(\frac{(n+1)K\rho_0^{(1-n)/n}}{4\pi G}\right)^{1/2} c^{(n+1)/n}, \tag{2.11}$$

and ξ is the 'dimensionless radius'. Thus, using chain rule, we find that

$$\frac{d\theta}{dr} = \frac{1}{a}\frac{d\theta}{d\xi} \quad and \quad \frac{d}{dr} = \frac{1}{a}\frac{d}{d\xi},$$

Inserting all of the above into eq. (2.10), and after performing algebraic manipulation, we reach

$$\frac{1}{\xi^2}\frac{d}{d\xi}\left(\xi^2\frac{d\theta}{d\xi}\right) = -\theta^n \tag{2.12}$$

the Lane-Emden equation, which is a dimensionless equivalent to the Poisson equation for Newtonian, spherically-symmetric polytropic fluids [8].

2.2.2 Obtaining the Chandrasekhar Mass

In this section, we will again closely follow the derivation from Sagert et al [5], with more detail. Having derived the Lane-Emden equation, we can now derive the Chandrasekhar mass - the largest mass a white dwarf can be. By Sagert et al [5], by integrating eq. (2.12) numerically, the solutions decrease with radius and have a zero at $\xi = \xi_1$, for which $\rho(r_1 = a\xi_1) = 0$. As such, the radius of the white dwarf is given by

$$R = \left(\frac{(n+1)K\rho_0^{(1-n)/n}}{4\pi G} \right)^{1/2} c^{(n+1)/n}\xi_1. \tag{2.13}$$

With this, we can now solve eq. (2.2), with eq. (2.13) being the upper limit; using eq. (2.9) and eq. (2.11), we obtain

$$\begin{aligned} M &= \int_0^R 4\pi r^2 \, dr \\ &= 4\pi a^3 \rho_0 \int_0^{\xi_1} \xi^2 \theta^n \, d\xi \end{aligned}$$

which we can derive the integral modifying eq. (2.12)

$$\xi^2 \left| \frac{d\theta}{d\xi} \right| = \int \theta^n \xi^2 \, d\xi,$$

to obtain

$$M = 4\pi c^{(2n+2)/(n+1)} \left(\frac{(n+1)K}{4\pi G} \right)^{(n)/(n-1)} \xi_1^{(n-3)/(1-n)} \xi_1^2 \left| \frac{d\theta}{d\xi} \right|_{\xi=\xi_1} R^{(3-n)/(1-n)}. \tag{2.14}$$

For the relativistic case, $\gamma = 4/3$ [9], so $n = 3$, and by Chandrasekhar, [10]

$$\xi_1 = 6.89685 \quad \text{and} \quad \xi_1^2 \left| \frac{d\theta}{d\xi} \right|_{\xi=\xi_1} = 2.01824$$

which by substituting into eq. (2.13) gives us

$$\mathrm{R} = \frac{\sqrt{3\pi}}{2}(6.89685) \left(\frac{\hbar^{3/2}}{\sqrt{G}c m_e m_N} \frac{Z}{A} \right) \left(\frac{\rho_{crit}}{\rho_0} \right)^{1/3}, \tag{2.15}$$

where

$$\rho_{crit} = \frac{m_N m_e^3 c^3}{3\pi^2 \hbar^3} \frac{A}{Z} \quad \text{and} \quad \rho_0 = \rho(r = 0).$$

Here, m_N is the nucleon mass, m_e is the electron mass and A/Z is the ratio between mass number and atomic number, which we assume is approximately 2 (considering the composition of a white dwarf.) We also note that the K in this case, for a relativistic white dwarf, is

$$K_{rel} = \frac{\hbar c}{12\pi^2} \left(\frac{3\pi^2}{2 m_n c^2} \right)^{4/3}. \tag{2.16}$$

Furthermore, we can also use the values to find the mass:

$$M = \frac{\sqrt{3\pi}}{2}(2.01824) \left(\frac{\hbar c}{G} \right)^{3/2} \left(\frac{Z}{m_N A} \right)^2,$$

which, after substituting numerical values, leads to [5]

$$\mathrm{M_{CH}} = 1.4312 \mathrm{M_\odot} \tag{2.17}$$

the Chandrasekhar mass, the largest possible mass for a white dwarf, using relativistic polytropic equations of state [11]. We will use these equations to later confirm the reliability of our computational methods.

2.3 General Relativity Correction

Near the Schwarzschild radius, as the star gets more compact, we must take into account the effects of general relativity due to the curvature of space-time. As such, we modify the ordinary differential equation for pressure. This is called the Tolman-Oppenheimer-Volkoff (TOV) equation. The TOV is given by [12–14]:

$$\frac{dp}{dr} = -\frac{G\epsilon(r)m(r)}{c^2r^2}\left[1+\frac{p(r)}{\epsilon(r)}\right]\left[1+\frac{4\pi r^3p(r)}{m(r)c^2}\right]\left[1-\frac{2Gm(r)}{c^2r}\right]^{-1} \tag{2.18}$$

We can see that the correction due to general relativity depends on the size of the star and its radius; by observation, it is apparent that the correction would be important for neutron stars, contrary to other celestial objects such as white dwarfs.

2.4 Fully Relativistic Case

In section 2.1, we have discussed the polytropic equation (2.4). The basis of this is the following equations, again assuming that the neutron star is entirely composed of Fermi gas of neutrons [5, 6]:

$$\epsilon(x) = \frac{\epsilon_0}{8}\left[(2x^3+x)(1+x^2)^{1/2} - \sinh^{-1}(x)\right] \tag{2.19}$$

$$p(x) = \frac{\epsilon_0}{24}\left[(2x^3-3x)(1+x^2)^{1/2} + 3\sinh^{-1}(x)\right] \tag{2.20}$$

where

$$\epsilon_0 = \frac{m_n^4c^5}{\pi^2\hbar^3} \quad \text{and} \quad x = \frac{k_F}{m_nc}.$$

k_F in this case is the Fermi momentum, which can be derived from Fermi energy. The Fermi energy is given by

$$E_F = \frac{\hbar}{2m_0}\left(\frac{3\pi^2\rho}{m_N}\frac{Z}{A}\right)^{2/3},$$

where m_0 is the fermion rest mass and m_N is the nucleon mass (neutron mass in the case of neutron stars); the rest have their usual meaning. Hence the Fermi momentum for neutron is

$$k_F = \sqrt{2m_0E_F} \quad \text{and} \quad k_F = \hbar\left(\frac{3\pi^2\rho}{m_N}\frac{Z}{A}\right)^{1/3},$$

where A/Z, naturally, has a value of 1.

For the polytropic case, following from the above, at the non-relativistic limit, these equations simplify to [5]

$$\epsilon(x) \simeq \frac{\epsilon_0}{3}x^3, \quad p(x) \simeq \frac{\epsilon_0}{15}x^5$$

and as such, we get eq. (2.4), with the K value being eq. (2.5). The K value for the relativistic case can be found similarly. However, for the fully relativistic case, we will not use the polytropic equation of state, but rather the full equations. This is further elaborated in section 3.2.2.

3 Computational Procedures

3.1 White Dwarfs

3.1.1 Finding the mass and radius

We begin the process by looking at white dwarfs, in order to check our computational methods and calculations with the simulation by Sagert et al [5]. Using a modified version of the Runge-Kutta algorithm

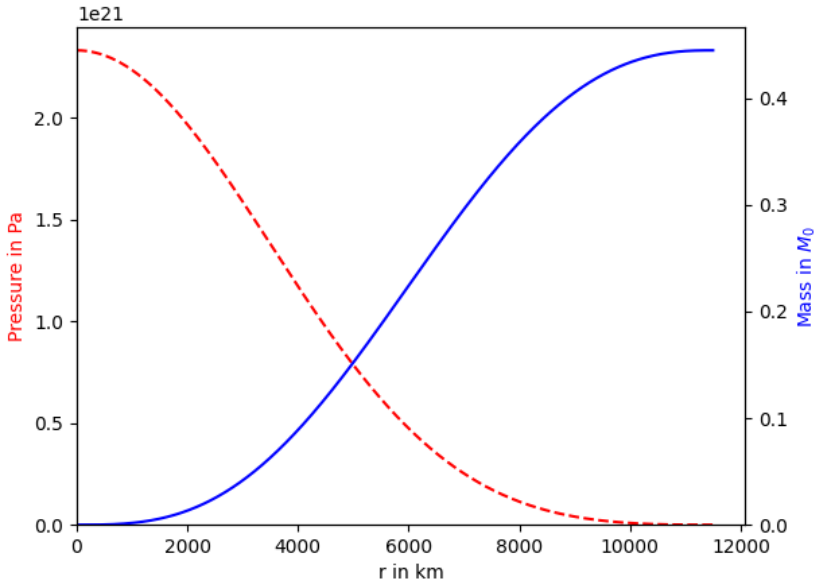

Figure 1: Plot of mass and pressure in terms of the radius of a non-relativistic white dwarf, $p_0 = 2.33002 \cdot 10^{21}$ Pa. The calculated radius and mass of the star are 11464 km and 0.44496 $M_\odot$ respectively.

so it accepts two coupled differential equations, (2.6) and (2.7), we can numerically solve these by setting initial boundary conditions - a central pressure value p_0 and $\bar{m}(0) = 0$.

The non-relativistic K value by the polytropic equation of state for white dwarfs, with $\gamma = 5/3$ is:

$$K_{non-rel} = \frac{\hbar^2}{15\pi^2 m_e} \left(\frac{3\pi^2}{2m_n c^2} \right)^{5/3} \tag{3.1}$$

Typically, due to the nature of the solution being numerical, a tolerance value is needed in order to find the radius of the star, as it is often the case that the pressure does not cross the zero to give us the value of the radius. However, due to artifacts of imaginary numbers which occur due to the algorithm, we were able to find the radius by finding the last term of the calculated list of values which is a real number in this case.

The values we obtained in this case, as shown in Fig.1, are R = 11,464 km and M = 0.44496 $M_\odot$ for a central pressure value of $p_0 = 2.33002 \cdot 10^{21}$ Pa. Comparing the calculated values with the reference [p.8] [5] which states that R = 10,919 km and M = 0.40362 $M_\odot$ we see that the results we have obtained are not exactly the same. However, we can assume that our simulation is correct - the general shape of the plot is the same, but there is only a slight variance in results compared to the reference.

We can repeat the process for the relativistic case, where $\gamma = 4/3$ and the K value is given by eq. (2.16), as shown in section 2.2.2. The result and the plot is shown in Fig.2; for a central pressure value of $p_0 = 5.62 \cdot 10^{24}$ Pa, we obtained R = 5710 km and M = 1.43134$M_\odot$. Comparing with the reference [p.9] [5], which states that R = 5710 km and M = 1.43145 $M_\odot$, we can see that the values are much more similar than the non-relativistic case. Furthermore, we note that the obtained value is very similar to that of eq. (2.17), the Chandrasekhar mass, which shows that our simulation for the initial pressure value is consistent with the theory.

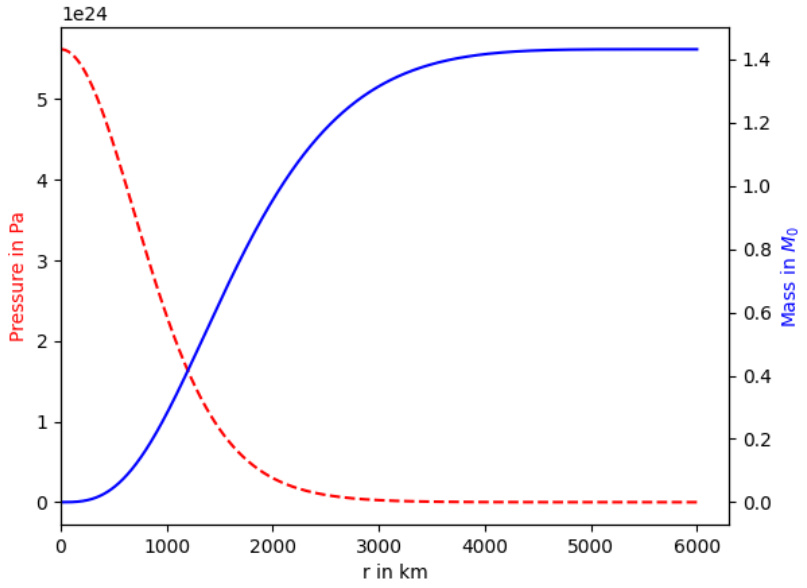

Figure 2: Plot of mass and pressure in terms of the radius of a relativistic white dwarf, $p_0 = 5.62 \cdot 10^{24}$ Pa. The calculated radius and mass of the star are 5710 km and 1.43134 $M_\odot$ respectively.

Iterating the above for both non-relativistic and relativistic cases many times, we can now plot the behaviour of the radius and mass of white dwarfs compared to their initial pressure. Fig.3 shows the non-relativistic case, while Fig.4 shows the relativistic case. The points plotted in Fig.4 (labelled R_{FIT}) are given by the equation (2.15), while the lines are calculated from equations, consistent with previous cases. From this, we can further confirm that the computational methods used are in accordance with the theoretical analysis.

3.2 Neutron Stars

3.2.1 Polytropic

We now move on to neutron stars, knowing that our calculations and graphical representation are consistent with reference [5]. We first explore the polytropic case; the computation is mostly the same as for the case of white dwarfs, but the K value is modified to the value in section 2.1, eq. (2.5).

Furthermore, we use the fact that $\epsilon(r) = \rho(r)c^2$; substituting this into eq. (2.4), we get the density in the form of:

$$\rho(r) = \left(\frac{p(r)}{Kc^{2\gamma}}\right)^{1/\gamma} \tag{3.2}$$

Inserting this into eq. (2.6) and eq. (2.7) for the Newtonian case and eq. (2.3) and eq. (2.18) for the TOV relativistic corrections, we can obtain Fig.5. We see that the difference between the Newtonian gravity and TOV correction gets larger for larger central pressure values; this shows the limitation of the Newtonian assumption.

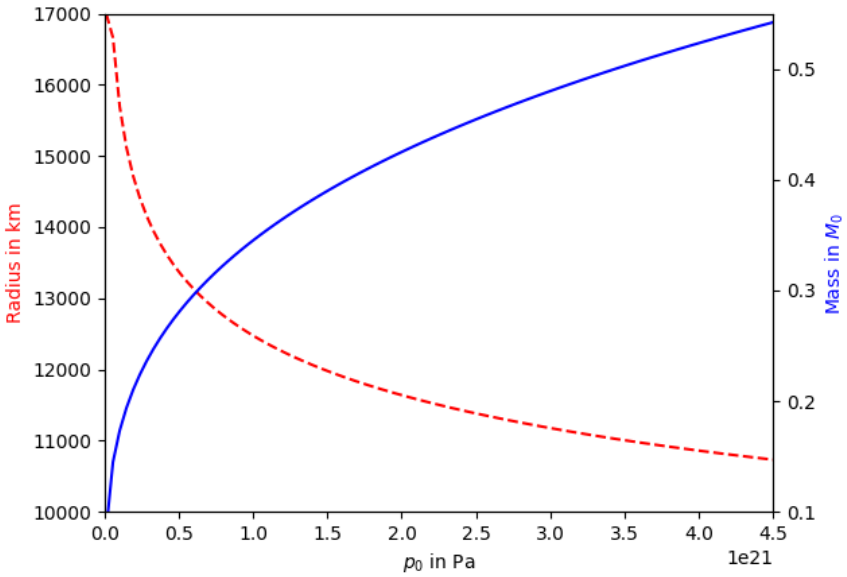

Figure 3: Plot of mass and radius in terms of the initial pressure of a non-relativistic white dwarf.

3.2.2 Fully relativistic

For the fully relativistic case, we can no longer use the polytropic assumptions; we must use the equations of pressure and energy density in terms of Fermi momentum, as shown in eq. (2.19) and eq. (2.20). Again, we reformulate the density:

$$\rho(r) = \frac{\epsilon(r)}{c^2}$$

which we can then use to redefine eq. (2.1) and eq. (2.3):

$$\frac{dm}{dr} = \frac{4\pi r^2 \epsilon(r)}{c^2} \quad \text{and} \quad \frac{dp}{dr} = -\frac{G\epsilon(r)m(r)}{c^2 r^2}.$$

Now we need to find the appropriate x value, which is in terms of the Fermi momentum k_F, for each point in the radius of the star after the initial pressure in order to calculate the full distribution of each neutron star for different initial pressure values. We do this by solving, for a given pressure value p in each iteration, the equation

$$p(x) - p = 0. \tag{3.3}$$

In order to be able to calculate the suitable x, we use the secant method as implemented in the function scipy.optimize.newton. The function itself is intended to use the Newton-Raphson algorithm, however, this is not the case here due to the fact that a derivative has not been stated explicitly. Nevertheless, the secant method was enough to produce satisfactory results. The step size of the Runge-Kutta also is a factor in making the algorithm work at higher orders of magnitude; the algorithm will fail to converge otherwise.

Furthermore, unlike the method used in section 3.1.1, we cannot take the final real pressure value anymore as the calculations do not produce complex numbers, seemingly due to the nature of the secant method.

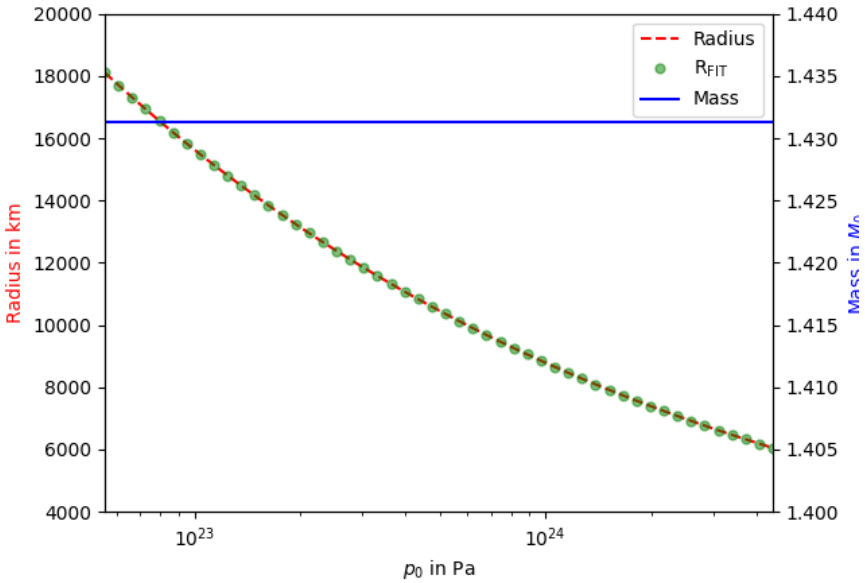

Figure 4: Plot of mass and radius in terms of the initial pressure of a relativistic white dwarf. Note that the x-axis is represented by a logarithmic base of 10.

Instead, as the calculated pressure values do cross zero, we take the last positive pressure value instead to find the radius and mass of the neutron star.

Obtaining the models of the neutron stars, we can plot them as below in Fig.6 and Fig.7.

We see that in Fig.6, there is a large fluctuation in the properties of the neutron stars for the fully relativistic case as the central pressure value increases. The neutron star with the largest mass is found at $p_0 = 3.6 \cdot 10^{34}$ Pa, with R = 9.14 km and M = 0.71 $M_\odot$ - similar to reference value [5] [p.16] (and that of Oppenheimer and Volkoff [12] [p.378]). This value has been confirmed using interpolation (interpolate.interp1d function on scipy.)

4 Conclusion

We were able to successfully model a neutron star's mass and pressure distribution depending on its radius given an initial pressure. The computational method was confirmed by applying it to white dwarfs to recover the Chandrasekhar limit.

We were also able to find the trend of the neutron star's radius and mass depending on the initial pressure. The star with the largest mass and radius was found to be at $p_0 = 3.6 \cdot 10^{34}$ Pa, with R = 9.14 km and M = 0.71 $M_\odot$, the Tolman-Oppenheimer-Volkoff limit for pure neutron stars [12], which is analogous to the Chandrasekhar limit for white dwarfs (although modern estimates consider the TOV limit to be $\sim 1.5 - 3.0 M_\odot$ [15].) This is in satisfactory agreement with our reference material by Sagert et al [5].

In terms of the method of computation, Brent's Method could have been used instead of the secant method for improved efficiency. However, as for each iteration of the Runge-Kutta the initial parameter of eq. (3.3) changes, it was difficult to find the required boundary conditions of the function for general

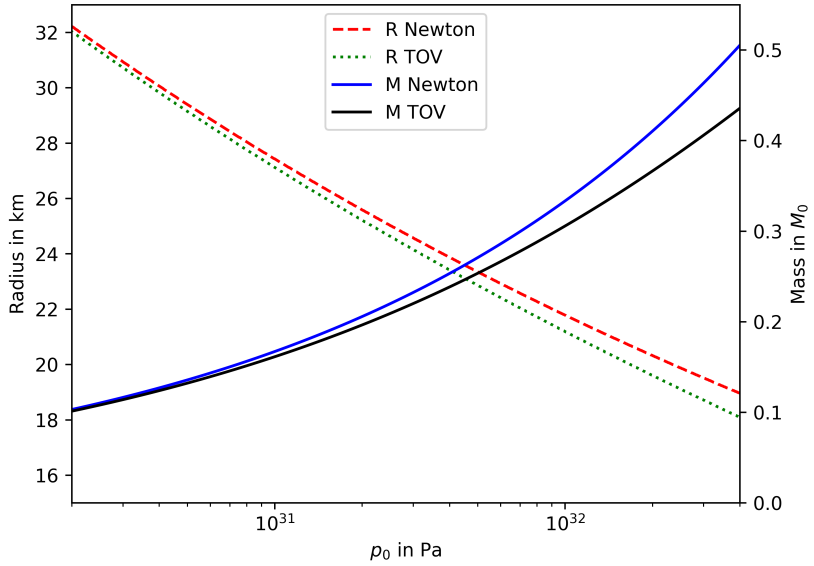

Figure 5: Plot of mass and radius in terms of the initial pressure for the Newtonian and TOV case of a Neutron Star, using the polytropic assumption in both cases. Note that the x-axis is represented by a logarithmic base of 10.

calculations (more specifically, the two boundaries on either side of the root.) Constructing a function to calculate these boundary conditions may have been an option, but after evaluating the computational speed for both methods at a set value of initial pressure, the difference was not drastic; we decided to use the secant method in the end as it produced satisfactory results. Nevertheless, for a more rigorous and larger range of calculations, Brent's method may be a better option.

As mentioned in section 3.2.2, the success in convergence for the secant method in the Newton-Raphson function depended on the step size used in the Runge-Kutta function. We found that having a smaller step size allowed for success in higher initial pressure values. As such, a more extensive list of neutron star properties can be determined when the step size is lowered. Furthermore, the numerical output would be more accurate to a larger significant figure. However, this also means that the computation would take much longer as we are essentially going through a larger number of calculations (especially while integrating the secant method.) Again, in the case of a more rigorous and extensive calculation, the step size should be lowered.

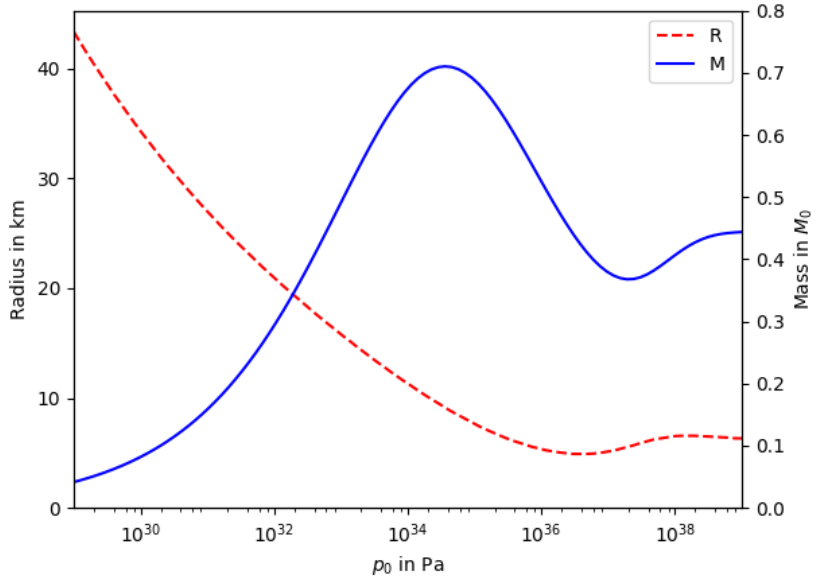

Figure 6: Plot of mass and radius in terms of the initial pressure for a pure neutron star, fully relativistic. The x-axis is represented by a logarithmic base of 10.

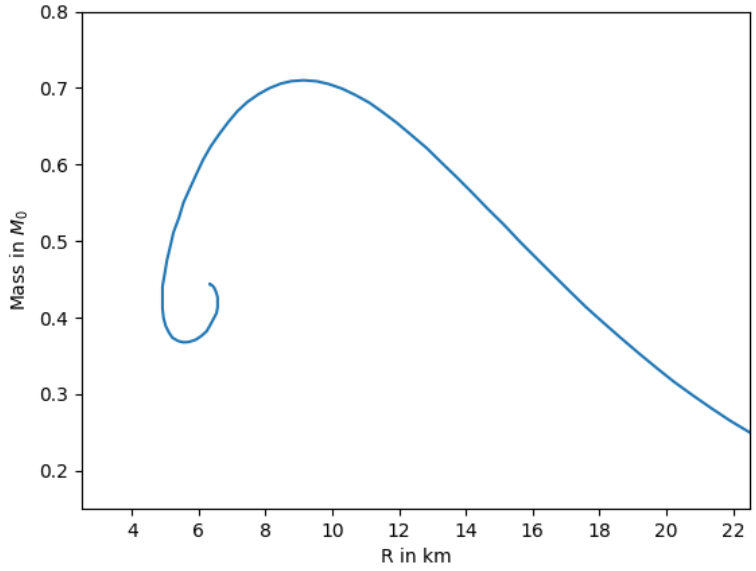

Figure 7: Plot of mass in terms of radius for each initial pressure value, for the fully relativistic Neutron Star.

References

[1] J. M. Lattimer and M. Prakash, "The physics of neutron stars," *Science*, vol. 304, no. 5670, pp. 536–542, 2004.

[2] C. R. Harris, K. J. Millman, S. J. van der Walt, R. Gommers, P. Virtanen, D. Cournapeau, E. Wieser, J. Taylor, S. Berg, N. J. Smith, R. Kern, M. Picus, S. Hoyer, M. H. van Kerkwijk, M. Brett, A. Haldane, J. F. del Río, M. Wiebe, P. Peterson, P. Gérard-Marchant, K. Sheppard, T. Reddy, W. Weckesser, H. Abbasi, C. Gohlke, and T. E. Oliphant, "Array programming with NumPy," *Nature*, vol. 585, pp. 357–362, Sept. 2020.

[3] P. Virtanen, R. Gommers, T. E. Oliphant, M. Haberland, T. Reddy, D. Cournapeau, E. Burovski, P. Peterson, W. Weckesser, J. Bright, S. J. van der Walt, M. Brett, J. Wilson, K. J. Millman, N. Mayorov, A. R. J. Nelson, E. Jones, R. Kern, E. Larson, C. J. Carey, İ. Polat, Y. Feng, E. W. Moore, J. VanderPlas, D. Laxalde, J. Perktold, R. Cimrman, I. Henriksen, E. A. Quintero, C. R. Harris, A. M. Archibald, A. H. Ribeiro, F. Pedregosa, P. van Mulbregt, and SciPy 1.0 Contributors, "SciPy 1.0: Fundamental Algorithms for Scientific Computing in Python," *Nature Methods*, vol. 17, pp. 261–272, 2020.

[4] J. D. Hunter, "Matplotlib: A 2d graphics environment," *Computing in Science & Engineering*, vol. 9, no. 3, pp. 90–95, 2007.

[5] I. Sagert, M. Hempel, C. Greiner, and J. Schaffner-Bielich, "Compact stars for undergraduates," *European Journal of Physics*, vol. 27, pp. 577–610, apr 2006.

[6] S. Balberg and S. L. Shapiro, "The properties of matter in white dwarfs and neutron stars," 2000.

[7] T. Hinderer, "Erratum: "tidal love numbers of neutron stars" (2008, apj, 677, 1216)," *The Astrophysical Journal*, vol. 697, p. 964, may 2009.

[8] S. Mukherjee, B. Roy, and P. Chatterjee, "Solution of lane-emden equation by differential transform method," *International Journal of Nonlinear Science*, vol. 12, 01 2011.

[9] M. Harwit, *Astrophysical Concepts*. Astronomy and Astrophysics Library, New York, NY: Springer New York, fourth edition ed., 2006.

[10] S. S. Chandrasekhar, *An introduction to the study of stellar structure*. New York: Dover Publications, 1957 - 1939.

[11] P. G. Frè, *Stellar Equilibrium: Newton's Theory, General Relativity, Quantum Mechanics*, pp. 237–271. Dordrecht: Springer Netherlands, 2013.

[12] J. R. Oppenheimer and G. M. Volkoff, "On massive neutron cores," *Phys. Rev.*, vol. 55, pp. 374–381, Feb 1939.

[13] W. Becker, *Neutron Stars and Pulsars*. Astrophysics and Space Science Library, 357, Berlin, Heidelberg: Springer Berlin Heidelberg, 2009.

[14] S. L. Shapiro, *Black holes, white dwarfs, and neutron stars : the physics of compact objects*. New York: Wiley, 1983.

[15] I. Bombaci, "The maximum mass of a neutron star.," *Astronomy and Astrophysics*, vol. 305, p. 871, Jan. 1996.